Modification of Aluminum Alloy 1933 by the High-Current Electron Beam Irradiation

A.G. Kobets[1, 2], P.R. Horodek[1], V.V. Lytvynenko[2], U.F. Lonin[3],
A.G. Ponomarev[3], O.A. Startsev[2,*], V.T. Uvarov[3]

[1] *JINR, 141980 Dubna, Moscow region, Russia*
[2] *Institute of Electrophysics and Radiation Technologies, National Academy of Sciences of Ukraine,*
28, Chernyshevsky Str., PO 8812, 61002 Kharkiv, Ukraine
[3] *National Science Center Kharkiv Institute of Physics and Technology,*
1, Akademichna Str., 61108 Kharkiv, Ukraine

Modification of the wrought aluminum alloy 1933 through irradiation by the intense microsecond relativistic hollow electron beam was studied. Fracture mechanisms for both irradiated and non-irradiated samples, changes in the structure and chemical composition were investigated. The thermal model describing the beam-metal interaction was developed based on the hyperbolic relaxation heat transfer equation, weakly coupled theory of thermoelasticity and Stefan problem. We used the finite difference method to perform calculations according to this model. We determined experimentally as well as numerically the areas of modified and non-irradiated material, localized the quenched, heat-affected and shock-wave-affected zones.

Keywords: Aluminum, Electron beam, Ablation.

1. INTRODUCTION

The effects observed during the interaction of high-current electron beams (HCEB) with metals and alloys are considered as a good basis to develop the new radiation nanotechnologies for surface modification in order to enhance physical and mechanical characteristics [1]. The modifying effect is achieved due to a great variety of different combined processes in the target: fast heating, melting, evaporation, elastic and shock wave formation and propagation, formation and expansion of gas plasma torch etc. The main feature of e-beam technologies that distinguishes them from the treatment methods based on impact by the other concentrated energy flows (lasers, plasma), is the maximum of energy deposition, which releases more deeply (related to the surface) in the bulk, than the others.

Industrial aluminum alloy 1933 of Al-Zn-Mg-Cu system was selected for study [2]. Nowadays, it is widely used because of it light density and high durability, typically it operates under cyclic loads [3]. Alloy 1933 has found numerous applications in the aircraft production of An-148, SSJ-100, as well as military aircraft and missile technology, significantly reducing the weight, fuel consumption, increasing weight efficiency of technology, its durability and service life. Alloys of the Al-Zn-Mg-Cu system are wrought alloys, and they are commonly used in quenched and artificially aged condition. These high-strength alloys have high vibration resistance, fatigue strength and favorably differ from other series of aluminum alloys [2]. On the other hand, these high strength alloys have bad weldability, ductility, malleability; it is also required to improve their crack and corrosion resistance. E-beam processing is one of possible ways to improve the physical and mechanical properties of alloy 1933. Moreover, to optimize the process of technological HCEB-processing it is im-portant to study in more detail the physical peculiarities of modifying mechanisms and develop the simple describing model.

2. MATERIALS AND METHODS

The irradiated sample was a square plate of aluminum alloy 1933 (6.35% Zn; 1.6% Mg; 1% Cu; 0.1% Mn; 0.2% Fe; 0.1% Si; 0.06% Ti; 0.05% Cr; 0.1% Zr; 0.0001% Be; the balance Al, % wt.) with the thickness ~ 2 mm and the side length ~ 10 mm [2]. One-impulse irradiation was conducted under the pressure about 10-5 Torr at the MIG-1 accelerator at the NSC Kharkiv Institute of Physics and Technology, with the following parameters: electron energy ~ 0.35 MeV, beam current ~ 2 kA, 5 µs beam pulse in the intensity range up to 10^{12} W/m². The pulse duration τ_{imp} was much longer that the electron–phonon relaxation time τ_r (10−11 s). The Gaussian-shaped hollow beam had the inner radius of 1.5 mm; the outer radius of 2.3 mm. Energy density released on the surface of the irradiated target was less than 5 MJ/m2. Linear dimensions of the plate were larger than the typical size of the interaction region.

Preliminary visual and morphological analysis of the irradiated sample was performed using the optical microscope Bresser BioLux NV. SEM, fractographic analysis and X-ray microanalysis were conducted using JEOL JSM-840. We also used the method of positron annihilation spectroscopy at LEPTA (JINR, Dubna, Russia) [4] to analyze the changes in the defect substructure. To conduct numerical calculations upon the stated below problem, the smoothing coefficients method was used. Numerical model based on Crank–Nicolson method was implemented in CodeTyphon 4.80, 64-bit Ubuntu 14.04 LTS.

---

* startsev-alex@ukr.net

3. RESULTS

3.1 Thermal Model of E-Beam Ablation

The mathematical model of evolution of the thermal field we build according to the relaxation model of the heat flux q and the temperature gradient ∇T (3.1), with a goal to describe physically correctly the propagation of the thermal front with a finite velocity and fulfill the maximum principle. We use the energy conservation equation (3.2), the power of internal heat source w is defined in (3.3). After substitution of (3.1) into (3.2) we obtain the hyperbolic heat conduction equation (3.4):

$$\vec{q}(\vec{r},t) = -\lambda \nabla T(\vec{r},t) - \tau_r \frac{\partial \vec{q}(\vec{r},t)}{\partial t} - \lambda \tau_r \nabla \frac{\partial T(\vec{r},t)}{\partial t} \,, \ (3.1)$$

$$\frac{\partial T(\vec{r},t)}{\partial t} = -\frac{1}{\rho c} div(\vec{q}) + \frac{w}{\rho c} \,, \qquad (3.2)$$

$$w(\vec{r},t) = \zeta \int j(\vec{r},t)S(\vec{r},t)d\vec{r}dt \,, \qquad (3.3)$$

$$\frac{\partial T}{\partial t} + \tau_r \frac{\partial^2 T}{\partial t^2} = \frac{\lambda}{\rho c}(\nabla^2 T + \tau_r \nabla^2 \frac{\partial T}{\partial t}) + \frac{w}{\rho c} + \frac{\tau_r}{\rho c}\frac{\partial w}{\partial t} \,, (3.4)$$

where λ – the coefficient of thermal conductivity, c – the thermal capacity, ρ – the material density, j – the beam current density, S – the energy-deposition profile [5], and the dimensional coefficient $\zeta = 1 \cdot 10^6$ J/MeV $\cdot$ C.

Then, we discretize our problem into two separate parts: on finding the temperature field and the thermo-mechanical part. We can apply the weakly coupled dynamic theory of thermoelasticity, taking into account the impact of the deformation rate $\dot{e}$ on the temperature increment $\dot{T}$, if the conditions (3.5 – 3.6) are fulfilled [3.6]:

$$\delta_0 = \frac{(3\lambda' + 2\mu')^2 a_T^2 T_0}{c\rho^2 \sqrt{\frac{\lambda' + 2\mu'}{\rho}}} \ll 1 \,, \qquad (3.5)$$

$$\frac{\dot{e}}{\dot{T}} \ll \frac{\alpha_T}{\delta_0}\frac{\lambda' + 2\mu'/3}{\lambda' + 2\mu'} \,, \qquad (3.6)$$

where λ', μ' – the Lame coefficients, α_T – the linear coefficient of thermal expansion. While the energy deposition S has a maximum at a depth about 120 µm, melting begins earlier in the bulk than on the surface (we do not consider the sublimation processes). The surface layer irradiated with a dose which is not enough for its melting, prevents the evaporation and ejection of the melted material at the mentioned depth under the surface. Consequently, it leads to the formation of the metastable phase in the volume (e.g. superheated liquid melt). The thermo-mechanical part considers the destruction of the aforementioned layer. It happens when the local ultimate strength Ω is equal to a jump of the mechanical tension $|\Xi|$. According to [3.6], we may simply estimate an upper bound of $|\Xi|$ using its normal-to-surface component σ_{zz}, which defines a tensile jump at the front of thermoelastic wave (3.7):

$$|\Xi| \sim \max(\sigma_{zz}) = (3\lambda' + 2\mu')\alpha_T(T(z,t) - T_0(z,0)) \,, (3.7)$$

The initial temperature is T_0. The boundary conditions are based on assumptions that the surface temperature at a remote, non-irradiated side is constant and equals to T_0

(3.8), but the incident surface is exposed to the intense irradiation which results in the multiphase transitions, melting, evaporation, thermal radiation and partial backward condensation of ejected material onto the target (3.9):

$$T\big|_{z\to\infty} = T_0 \,, \qquad (3.8)$$

$$\lambda \frac{\partial T}{\partial r}\Big|_{z=0} + \beta T\big|_{z=0} + n^2 \sigma \varepsilon_R T^4\big|_{z=0} = q_{surf}^{beam} + q^{cond} \,, (3.9)$$

where β – the heat transfer coefficient, ε_R – the integral emissivity, n – the refractive index of the environment ($n \approx 1$). q_{surf}^{beam} denotes the heat flux per unit area absorbed by the target (3.10), q^{cond} describes an amount of heat released during the backward condensation of ablation products onto the surface (3.11 – 3.12):

$$q_{surf}^{beam} \approx \zeta \int j(r,t)S(r)dzdt \,, \qquad (3.10)$$

$$m_{abl} \approx \int \rho dV\big|_{T > Tmelt} \,, \qquad (3.11)$$

$$q^{cond} \approx \theta m_{abl}(c(T_{melt} - T_o) + \sum_k L_k)j(t)e^{-\frac{(t-\varphi)^2}{2D}} \,, (3.12)$$

where m_{abl} – the ablated mass, T_{melt} – the melting temperature, θ – the condensation coefficient ($\theta \sim 1/6$), L_k – the latent heat per unit of volume, $D = 1$ s^{-2}, φ – a parameter, which denotes a delaytime of the condensation on the target surface relatively to the beginning of irradiation ($\varphi \sim \tau_{imp}/2$). At the moving boundary of phase transition we also set the next conditions (3.13 – 3.14):

$$T_{j-1}(\xi - 0,t) - T_j(\xi + 0,t) = T_{tran,k} \,, \qquad (3.13)$$

$$\lambda_{j-1}\frac{\partial T_{j-1}}{\partial r} - \lambda_j \frac{\partial T_j}{\partial r} = L_k \rho \frac{d\xi}{dt} \,, \qquad (3.14)$$

where ξ – the front of k-phase transition, which occurs at the transition temperature $T_{tran,k}$.

3.2 Experimental and numerical results

Experimental results showed that HCEB irradiation caused significant erosion to sample. The nature of sample cross-fractures was investigated. It was found that the modified volume consists of the quenched zone (QZ), heat-affected (HAZ) and shock-wave-affected zones (SWZ) differed one form each other by their microstructure, chemical composition, fracture mechanisms (Fig. 1), concentration and kinds of defects. However, we have not noticed the considerable differences between HAZ and SWZ due to the annealing effect of e-beam processing, thus we considered those two zones as one. QZ has the closely packed, highly disperse nonporous structure, which consists of misoriented grains with linear dimensions in rage of $1 - 3$ µm, its fracture is dimpled and quasi-fibrous. QZ with a thickness about 200 µm was formed as a result of the high-speed cooling and the backward condensation of ablated material. HAZ and SWZ with a thickness up to 400 µm were formed due to the influence of rapid thermal fixation of the shock-wave effect on the melt. It is characterized by the micro-ductile fracture mechanism and nonporous fine structure of highly melted facets with a linear size 1 µm without any specific orientation. Non-modified alloy is characterized by the well-organized structure of quasi-cleavage crack facets within the size interval $0.6 - 1.5$ µm.

The results obtained numerically according to the developed thermal model are in good agreement with the experimental data. We obtain numerically the penetration depth into the sample and it is not more than 0.8 mm at the irradiation epicenter (peak flux density of up to 10^9 W/sm^2). The microstructure of the modified alloy depends on the heating and cooling rates (Rht, Rcl), on the corresponding temperature gradients (Ght, Gcl), which in turn depend on the heat and mass transfer in the system, which finally influences on the alloy composition. The computed heating rate $Rht \sim 10^8 - 10^9$ K/s and the heating gradient $Ght \sim 10^6 - 10^8$ K/m in the near-surface region (less than 200 µm). The thickness of the quenched layer does not exceed 300 µm in the peripheral regions (flux densities up to 10^6 W/sm^2) and $100 - 200$ µm at the irradiation epicenter, the cooling rate and temperature gradient $Rcl \sim 10^7 - 10^8$ K/s and $Gcl \sim 10^7 - 10^8$ K/m respectively. The thickness of the melting and shock-wave-affected zone is up to 500 µm at the depth of $600 - 800$ µm relatively to the surface, $Rcl \sim 10^4 - 10^6$ K/s and $Gcl \sim 10^3 - 10^5$ K/m. Evolution of the ablation interface is characterized by some impulsiveness due to the inhomogeneous volumetric heat dissipation and localization of stresses. The temperature maximum in the bulk eventually disappears, and the crater is broadened. After $2 - 3$ µs the temperature maximum moves almost onto the surface, and the velocity of the interface between the modified and non-treated material goes in the stationary mode 100 m/s.

EPMA of the sample showed a substantial enrichment (20%) by the major alloying elements Zn, Mg and Cu in the quenched zone at the depth to 120 µm with the maximal concentrations at the surface; probably this effect occurred due to the diffusion of fusible compounds onto the surface. We also conducted EPA analysis of our samples (Fig. 2). At the beginning the Doppler parameter s increases linearly with E (i.e. with depth) describing by that way a presence of the oxide layer on the surface. The large peak in the interval 2-10 keV showed a decline in the degree of crystallinity (little amorphization) which might be caused by the accumulation of any kind defects, redistribution of alloying elements, relaxation of high residual stresses near the surface. It should be noted, that such a phenomenon could not be caused by the influence of the elastic, shock waves, since all the investigated volume was formed during the fast crystallization of the melt after the irradiation. Recrystallization processes formed almost all the modified structure, as evidenced by the small change of s-parameter. The e-beam irradiation affected the type of defects towards increasing the number of vacancy defects, as indicated by the change in slopes of the straight lines.
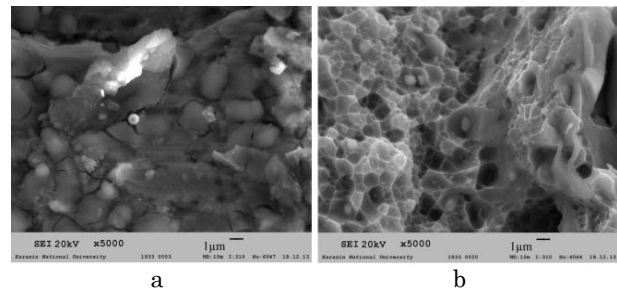
Fig. 1 – Fractures of irradiated material in QZ (a) and (b) non-irradiated material.
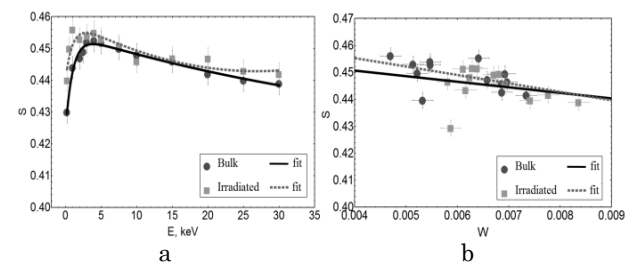
Fig. 2 – Dependences of s-parameter on E positron energy (a) and s-parameter on w-parameter (b) for unmodified bulk and irradiated (in HAZ and SWZ area) alloy 1933.

4. CONCLUSIONS

The modification of industrial aluminum alloy 1933 by the high-current electron beam was studied. The thermal model was developed correspondingly. The e-beam irradiation resulted in a significant enrichment of alloying elements Mg, Zn, Cu in the subsurface quenched zone, compared to non-irradiated sample. The topological changes of fracture from the quasi-cleavage crack facets in the unmodified area to tearing dimples, to highly melted facets in the transition zone, and dimpled, dull, quasi-fibrous fracture in the quenched zone were observed. It was proved that the HCEB treatment increased the proportion of micro-ductile fracture of aluminum alloy 1933.

REFERENCES

1. V.I. Boiko, A.N. Valyaev, A.D. Pogrebnyak, *Sov. Phys. Usp.* **169**, 11 (1999).
2. *Aluminum Alloys* (Ed. I.N. Fridlyander) (Kiev: Komintech: 2005).
3. V.P. Poida, D.E. Pedun, V.V. Bryukhovetskii, A.V. Poida, R.V. Sukhov, A.L. Samsonik, V.V. Litvinenko, *Phys. Met. Metallogr.* **114**, 9 (2013).
4. P. Horodek, A. Kobets, I. Meshkov, V. Pavlov, A. Rudakov, A. Sidorin, S. Yakovenko, *Proc. RUPAC2012,* WEPPC044 (2012).
5. V. Gann, H. den Hartog, A. Sugonyako, D. Vainshtein, *Proc. EPAC 2004*, 2756 (2004).
6. E.M. Kartashov, L.M. Ozherelkova, *Matematicheskoe Modelirovanie* **14**, 2 (2002).